Conference Paper

A Test Rig for the Calibration of Strain Sensing Carbon Fibre

Durieux, O., Day, R.J., Vagapov, Y.

This is a paper presented at the 3rd Int. Conf. on Communication, Computing and Industry 4.0, Bangalore, India, 15-16 Dec. 2022

A Test Rig for the Calibration of Strain Sensing Carbon Fibre

Olivier Durieux
Faculty of Art, Science and Technology
Glyndwr University
Wrexham, UK

Richard J. Day
Faculty of Art, Science and Technology
Glyndwr University
Wrexham, UK

Yuriy Vagapov
Faculty of Art, Science and Technology
Glyndwr University
Wrexham, UK

***Abstract*—This paper presents the test equipment developed for the measurement and calibration of sensing carbon fibre. The testing device provides precise load application to a carbon fibre tow and measuring the micro-variations of the fibre electrical resistance in a temperature-controlled environment. The measurement approach based on sensing carbon fibre is a method for strain measurement being recently developed and similar to the traditional strain gauge method. However, due to the integration of the sensing element into the material, it is considered the most promising alternative for carbon fibre reinforced plastic applications. The theory behind fibre strain measurement including the influence of the temperature on the fibre electrical resistance is presented. A detailed presentation of the measurement and calibration device is given including the measurement loop. The test rig is capable of testing fibres at a temperature up to 180°C and the maximum load applied to the fibre of 1500N. A 5-run test on a T300 3K carbon fibre at 100°C is provided as an example of the test rig operation. On average, the accuracy of the testing method over half load (700N) offers results having a maximum variation of 5% around the mean value of the whole set of test readings collected.**

Keywords—carbon fibre, sensing fibre, strain, CFRP, test rig, measurement

I. Introduction

Measuring the strain in materials has always played a vital role in the determination of the stress in materials allowing the assessment of ultimate capacity, low-cycle fatigue, and service life of components. In other words, strain is a key factor in component design [1]. This rationale is particularly crucial for complex parts manufactured using innovative materials such as carbon fibre reinforced plastic (CFRP) produced by traditional cure techniques or innovative microwave cure techniques [2].

The measuring technique discussed in this paper has been developed primary for CFRP-based material although it allows the calibration of any sensing fibre. The calibrated sensing fibre can be used in many other applications including smart clothing, sensing matrices, concrete deformation measurement, etc. [3]-[9].

Strain is often measured using both extensometers and traditional techniques (there are many other techniques, but field applications are limited). The advantages of the fibre sensing technique over existing techniques are: (1) it is simple to use or implement when the part is in use, (2) it is accurate and reliable at all temperatures, (3) it requires low-cost investment as well as low cost per measurement point, (4) it is non-destructive nor intrusive (affecting the integrity of the CFRP due to their size or connectivity), (5) it is suitable for surface as well as internal, measurement of the strain.

The aim of the device presented in this paper is to provide a quick and accurate measurement of the variation of resistance and inductance of currently available carbon fibre. It can be used to develop the innovative strain measurement technique using carbon fibre as a sensor in the application fields listed above. To be valuable and innovative, the measurement technique, once fully developed, should satisfy the following requirements: (1) the measurement technique should provide a good sensibility to strain during the cure and service of the part (0.5με), (2) it should ensure good repeatability (and reproducibility) (less than 0.5%), (3) the technique has to be simple in terms of connection and measurement. In addition, the strain measurement technique should not interfere with the integrity of the material nor create any chemical interference with the matrix or the resin used.

The most suitable solution to meet the above requirements appears to be to use carbon fibres as sensors. In fact, carbon is a conductive material that has conductivity characteristics in line with all other conductors including temperature changes [3],[10]-[14].

II. Theoretical Background

A. Elastic Strain in Conductive Fibres

The basic principle of strain measurement using a conductive fibre is, in all logic, associated with the elastic change in length of the fibres in the direction of the strain.

Let OA be the unstrained fibre, $O'A'$ the ends of the strained fibre, x the direction, and ΔOA_x the overall change in length of the fibre due to strain (Fig. 1). It can be written that:

$$\Delta OA_x = \left(x_{A'} - x_{O'}\right) - \left(x_A - x_O\right) = \\ = \left[\left(dx + u + \frac{\partial u}{\partial x}dx\right) - u\right] - \left(dx - 0\right) = \frac{\partial u}{\partial x}dx \quad (1)$$

Elastic Strain (ε) is defined as the extension per unit length. Elastic Strain (ε_{xx}) of the fibre OA having a length OA in the x direction and written as:

$$\varepsilon_{xx} = \frac{\Delta OA_x}{dx} = \frac{\frac{\partial u}{\partial x}dx}{dx} = \frac{\partial u}{\partial x} \quad (2)$$

Elastic Strain (ε_{xx}) of a material is equal to the local displacement of any reference point in the x direction. Elastic tensile and compressive stresses (σ) are defined as the amount of tensile or compressive force (F) per unit area of the cross section subjected to stress (A). The ability of a material to withstand changes in length under tensile and compressive stress is Young's modulus (E). Young's modulus is defined in the elastic domain of any material as the longitudinal stress divided by the strain $E = \sigma/\varepsilon$. The value of Young's modulus varies with the interatomic bonding of the atoms constituting the material. The modulus of carbon fibre is typically 230 GPa and its ultimate tensile strength is typically 3.5 GPa.

The majority of the engineering materials experience a decrease in Young's modulus with temperature. The temperature dependence of the elastic stiffness constants of

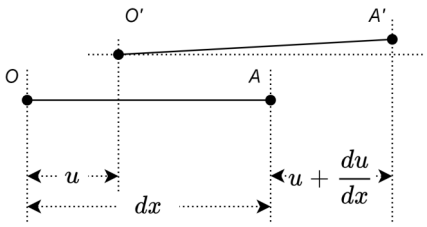

Fig. 1. 2d principle of fibre elongation.

most traditional engineering materials is a well-known phenomenon linked to their melting temperature (T_m). Experimental data are generally used to qualify the variation. For ceramics, the following empirical formulas can be used to determine Young's modulus at any temperature T (for $T < 0.5\ T_m$) as rough estimates [15]:

$$E_T = E_{0K}\left(1 - a\frac{T}{T_m}\right) \tag{3}$$

where E_{0K} is Young's modulus of the material at 0K, T_m is the melting temperature of the material in K, a is a coefficient equal to 0.3 for ceramics (0.5 for metals).

There is another important elastic constant that should be taken into consideration in the context of this study. This is, for every material, a constant that characterises the ratio of transverse strain to axial strain. It is commonly called Poisson's ratio and is denoted v. In the context of a conductive fibre, considering a unique longitudinal strain ε_L applied to a unit volume of material along the x direction, the Poisson's ratio gives:

$$v = -\frac{\varepsilon_T}{\varepsilon_L} \quad \text{or} \quad \varepsilon_T = -v\varepsilon_L \tag{4}$$

The transversal strain on the fibre (noted ε_T) has an important effect on the cross-section of the fibre and influences the overall electrical resistance per unit of length of it.

B. *Electrical Resistance Changes due to Strain and Temperature*

The length, cross-sectional area, and resistivity are the elements that affect the resistance of a conductor. The resistance of a conductor (R) is given by the relation

$$R = \rho_t \frac{L}{S} \tag{5}$$

where ρ_t is the resistivity at temperature T, L is the length, S is the cross-sectional area.

As mentioned above, the elastic strain (ε_{xx}) of the OA having a length dx in the direction x is defined as

$$\varepsilon_{xx} = \frac{\partial u}{\partial x} = \sigma_{xx}E^{-1} \tag{6}$$

Taking into consideration the lateral strains induced by the longitudinal strain:

$$\varepsilon_{yy} = \varepsilon_{zz} = -v\varepsilon_{xx} = -v\sigma_{xx}E^{-1} \tag{7}$$

In the context of the resistance of a conductor having a length L, a diameter D, and subjected to a longitudinal stress σ_{xx} (generating strains ε_{xx}, ε_{yy}, and ε_{zz}), the resistance under stress $R_{Stressed}$ can be expressed as

$$\begin{aligned} R_{Stressed} &= \rho_t \frac{L_{Stressed}}{S_{Stressed}} = \rho_t \frac{L_{Stressed}}{\pi D^2_{Stressed}} = \\ &= \rho_t \frac{L\left(1+\varepsilon_{xx}\right)}{\pi D^2\left(1+\varepsilon_{yy}\right)^2} \end{aligned} \tag{8}$$

Applying Poisson's theory and the elasticity principles to the relation gives the following.

$$R_{Stressed} = \rho_t \frac{L\left(1+\varepsilon_{xx}\right)}{\pi D^2\left(1-v\varepsilon_{xx}\right)^2} = \rho_t \frac{L\left(1+\sigma_{xx}E^{-1}\right)}{\pi D^2\left(1-v\sigma_{xx}E^{-1}\right)^2} \tag{9}$$

Considering that the resistivity for the material at temperature T is constant when subjected to stress, the relationship can be rewritten as

$$dR = R - R_{Stressed} = \rho_t \frac{L}{S} - \rho_t \frac{L_{Sressed}}{\pi D^2_{Stressed}} = \rho_t\left(\frac{L}{S} - \frac{L+dL}{S+dS}\right) \tag{10}$$

where d is the change in value due to strain.

Taking into account small changes in value due to strain, it is possible to approximate the equation. The relation can then be rewritten as

$$dR = \rho_t d\left(\frac{L}{S}\right) \tag{11}$$

or

$$\ln\left(R\right) = \ln\left(L\right) - \ln\left(S\right) \tag{12}$$

and

$$\frac{dR}{R} = \frac{dL}{L} - \frac{dS}{S} \tag{13}$$

It is now possible to identify ε_{xx} in the above equation since $\varepsilon_{xx} = dL/L$. Using the same approach, it is possible to announce that

$$\frac{dD}{D} = \varepsilon_{yy} = -v\varepsilon_{xx} \tag{14}$$

Furthermore, cross section S is equal to πD^2. Therefore, it is possible to write that

$$\frac{dS}{S} = 2\frac{dD}{D} \quad \text{or} \quad \frac{dS}{S} = 2\varepsilon_{yy} = -2v\varepsilon_{xx} \tag{15}$$

Substituting (15) into (13):

$$\frac{dR}{R} = \varepsilon_{xx} - \left(-2v\varepsilon_{xx}\right) = \varepsilon_{xx}\left(1+2v\right) \tag{16}$$

The variation in resistance dR/R is therefore proportional to the longitudinal strain ε_{xx}.

The proportionality coefficient between dR/R and the strain ε_{xx} is $(1 + 2v)$ and is defined as the gauge factor (GF), so,

$$\frac{dR}{R} = \varepsilon_{xx}GF \tag{17}$$

and

$$GF = \frac{dR/R}{\varepsilon_{xx}} = 1 + 2v \tag{18}$$

If the resistivity for the material when subjected to temperature is changing, then it is required to include the previously detailed relation between resistivity and temperature for the determination of the GF. The resistivity relation can be rewritten as

$$\rho_t = \rho_0\left[1+\alpha\left(T-T_0\right)\right] = \rho_0 + \rho_0\alpha T - \rho_0\alpha T_0 \tag{19}$$

where ρ_0 is the resistivity at temperature T_0, α is the coefficient of resistivity.

For a change of temperature dT between the temperatures T_1 and T_2, the variation of resistivity $d\rho_t$ is:

$$\begin{aligned} d\rho_t &= \left(\rho_0 + \rho_0\alpha T_2 - \rho_0\alpha T_0\right) - \left(\rho_0 + \rho_0\alpha T_1 - \rho_0\alpha T_0\right) = \\ &= \rho_0\alpha\left(T_2 - T_1\right) = \rho_0\alpha dT \end{aligned} \tag{20}$$

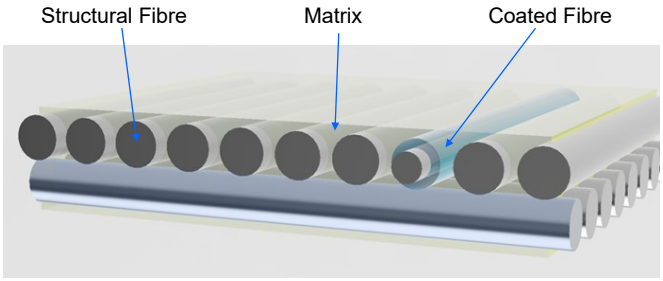

Fig. 2. Embedded system of strain measurement in CFRP.

The overall change of resistance due to strain and temperature (11), (12) and (13) can be rewritten as

$$\ln(R) = \ln(\rho_t) + \ln(L) - \ln(S) \tag{21}$$

subsequently,

$$\frac{dR}{R} = \frac{d\rho_t}{\rho_t} + \frac{dL}{L} - \frac{dS}{S} \tag{22}$$

The quantity $d\rho_t/\rho_t$ may be the result of temperature and strain. Therefore, the identification of the gauge factor GF can be split into:

$$\frac{dR}{R} = \frac{dL}{L} - \frac{dS}{S} + \left[\frac{\rho_0 \alpha dT}{\rho_0 \alpha (T - T_0)} + \frac{d\rho_t}{\rho_t}_{Strain} \right] \tag{23}$$

$$GF = 1 + 2v + \frac{dT}{T - T_0} + \frac{d\rho_t/\rho_t}{\varepsilon_{xx}} \tag{24}$$

The influence of the change in resistance due to temperature $dT/(T - T_0)$ can be important. It is, however, extremely predictable, and its influence on measurement can be easily taken into consideration.

III. Existing Techniques of Strain Measurement Applicable to CFRP

As previously demonstrated, the nature and temperature sensitivity have a significant influence on the electrical conductivity of the sensing fibres. Understanding these characteristics is essential to developing a fully embedded system of strain measurement in CFRP, as shown in Fig. 2.

Currently, many strain measurements are available. The traditional strain gauge is probably the most used solution to measure strain. It is a well-developed technique that offers many advantages for surface measurement. It is unfortunately inappropriate for internal strain determination since the gauge and its associated wiring can alter the integrity of the measured structure. Photoelasticity, fibre optics, and Raman-based spectroscopy are techniques that have also demonstrated their capabilities in extensiometry. However, none of them has the capabilities of offering a solution that is suitable for simultaneously (1) creating no interference with the part measured, (2) simple and suitable for out-of-the-lab applications, and (3) being cheap to implement and maintain in field applications for CFRP.

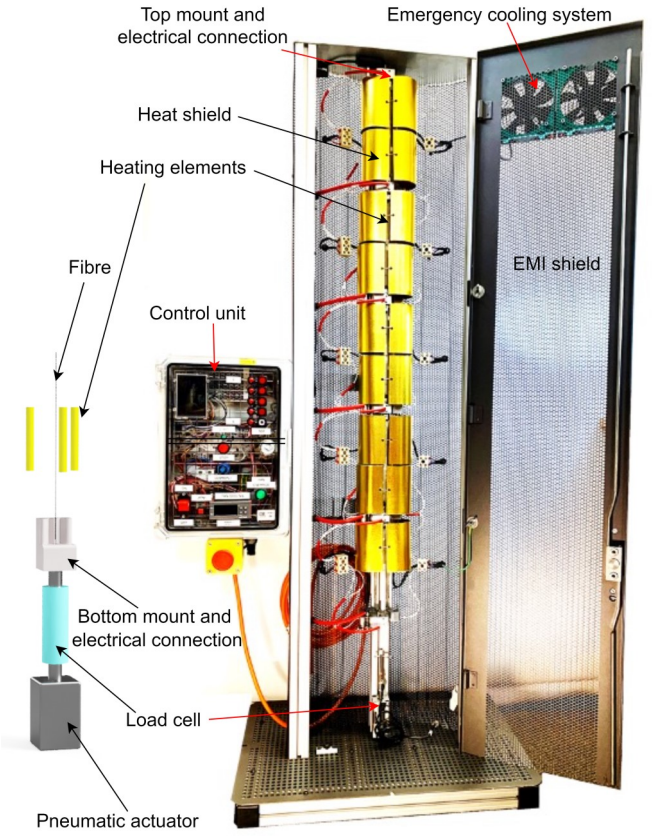

Fig. 3. Test rig.

The implementation of a sensing fibre when stacking the layers of carbon fibre has not currently been overlooked, but it is predicted that it should not be a significant issue due to the absence of variation of size between bearing and measuring tows. The characterization of the fibre under strain under various temperature conditions is a critical element of the development; the EMC-protected test rig allowing for the latter characterisation is explained below.

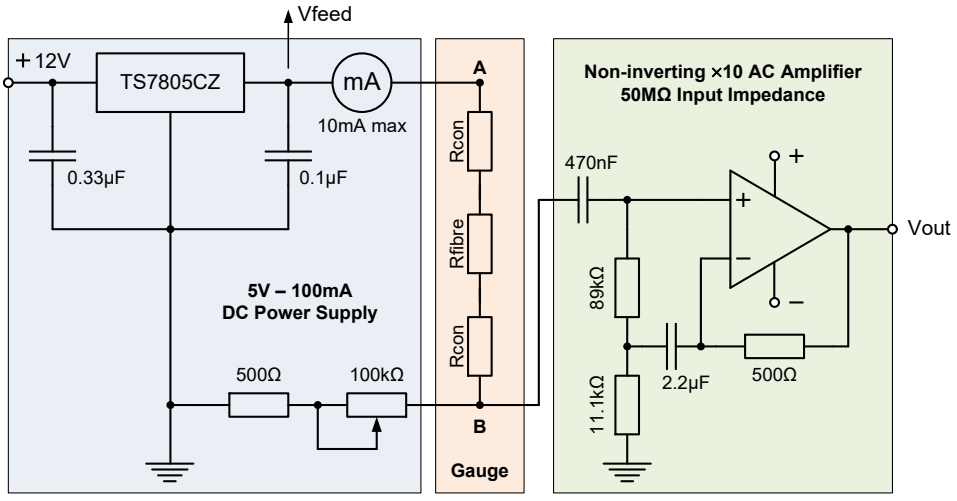

Fig. 4. PSU/AO measurement loop.

TABLE I. 5 RUNS ON T300 3K FIBRE AT 100°C

	run #1			run #2			run #3			run #4			run #5		
Target (N)	Measured Load (N)	$R-R_0$ $10^{-6}\Omega$	$(R-R_0)/L$	Measured Load (N)	$R-R_0$ $10^{-6}\Omega$	$(R-R_0)/L$	Measured Load (N)	$R-R_0$ $10^{-6}\Omega$	$(R-R_0)/L$	Measured Load (N)	$R-R_0$ $10^{-6}\Omega$	$(R-R_0)/L$	Measured Load (N)	$R-R_0$ $10^{-6}\Omega$	$(R-R_0)/L$
100	100.6	0.16	0.00159	99.3	0.15	0.00151	99.5	0.16	0.00161	100.8	0.18	0.00179	100.7	0.16	0.00164
300	302.8	0.47	0.00155	300.5	0.47	0.00155	300.6	0.46	0.00152	299.5	0.45	0.00149	302.9	0.44	0.00145
500	502.3	0.89	0.00177	503.6	0.90	0.00179	498.7	0.92	0.00184	495.6	0.94	0.00190	500.0	0.95	0.00190
700	699.3	1.12	0.00160	704.7	1.12	0.00159	701.8	1.10	0.00157	696.4	1.12	0.00161	702.4	1.09	0.00156
900	896.3	1.58	0.00176	908.0	1.50	0.00165	897.8	1.52	0.00169	891.5	1.53	0.00172	899.7	1.50	0.00167
1100	1099	1.72	0.00156	1094	1.75	0.00160	1094	1.75	0.00160	1091	1.78	0.00163	1105	1.76	0.00160
1300	1288	2.02	0.00157	1293	2.02	0.00157	1304	2.00	0.00154	1290	2.04	0.00158	1301	2.04	0.00157
1500	1501	2.57	0.00171	1495	2.58	0.00173	1495	2.40	0.00161	1494	2.41	0.00161	1502	2.38	0.00159
1300	1293	2.04	0.00158	1300	2.02	0.00155	1302	1.99	0.00153	1297	2.00	0.00154	1308	2.00	0.00153
1100	1093	1.71	0.00157	1092	1.71	0.00156	1094	1.71	0.00157	1102	1.69	0.00154	1097	1.55	0.00141
900	893.2	1.42	0.00159	902.8	1.40	0.00155	897.9	1.40	0.00156	906.8	1.39	0.00153	898.3	1.39	0.00155
700	698.8	1.09	0.00156	693.3	1.12	0.00161	694.0	1.10	0.00158	697.0	1.11	0.00160	696.5	1.12	0.00160
500	500.6	0.87	0.00174	501.3	0.87	0.00174	499.1	0.89	0.00179	500.7	0.91	0.00183	499.5	0.91	0.00182
300	298.0	0.48	0.00161	301.1	0.47	0.00155	298.8	0.48	0.00162	300.4	0.47	0.00156	299.7	0.49	0.00163
100	99.7	0.18	0.00181	100.9	0.16	0.00160	99.2	0.14	0.00144	99.9	0.16	0.00158	101.0	0.18	0.00178
0	0.0	0.00	/	0.0	0.00	/	0.0	0.00	/	0.0	0.00	/	0.0	0.00	/
		mean	0.00164		mean	0.00161		mean	0.00161		mean	0.00163		mean	0.00162
		max	0.00181		max	0.00179		max	0.00184		max	0.00190		max	0.00190
		min	0.00155		min	0.00151		min	0.00144		min	0.00149		min	0.00141
	Std Deviation		0.00009	Std Deviation		0.00008	Std Deviation		0.00010	Std Deviation		0.00012	Std Deviation		0.00013

IV. TEST RIG

A. Rig Description

The characterisation rig presented below allows a fibre of up to 1m to be placed under stress – the stress is generated by a pneumatic actuator. This allows unnecessary EMC to be avoided. Full details are shown in Fig. 3.

The stress is measured using a calibrated load cell allowing the strain to be determined using the previously developed relations. The orientation of the fibre (vertical) allows for avoiding any bending of the fibre under its own weight.

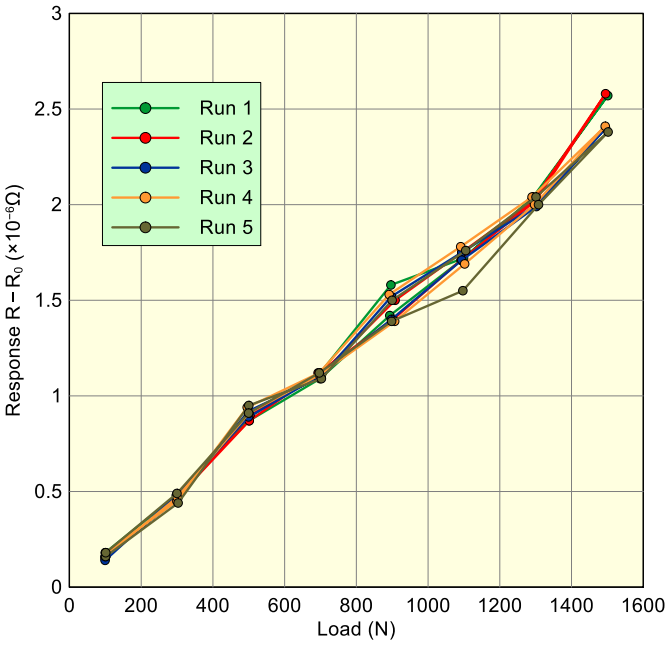

Fig. 5. Variation of the response in 10^{-6} Ω of a T300 3K 1000mm fibre versus load at 100°C.

The temperature is applied using Phillips IR bulbs (3 bulbs equally positioned around the fibre) in sections of 20cm, each section totalising 900W of heating capacity. Heat is maintained using plain insulated shields and controlled along the fibre using PT100 RDT sensors. The temperature management is separated into five zones to compensate for the temperature differences along the fibre (due to the stack effect – heat going up). Bulbs are isolated and earthed when measurements are taken, and EMI/RFI are avoided using a generic mesh shield around the system. Safety features include cooling fans automatically actuated when the temperature of the top of the structure is reaching levels over 150°C.

The resistance of the fibre (including the resistance of the connections and leads) can be measured using an LCR meter and 4-wire probe; it can also be measured using a non -inverting amplifier (high inductance) and an accurate PSU

TABLE II. ANALYSIS OF THE DISCREPANCY IN THE MEASUREMENT OF $(R-R_0)/L$ OF A T300 3K 1000MM FIBRE

	$(R-R_0)/L$			
Target (N)	mean	max	min	Std Deviation
100	0.0016	0.0018	0.0015	-0.00010
300	0.0015	0.0016	0.0015	-0.00004
500	0.0018	0.0019	0.0018	-0.00006
700	0.0016	0.0016	0.0016	-0.00002
900	0.0017	0.0018	0.0017	-0.00004
1100	0.0016	0.0016	0.0016	-0.00002
1300	0.0016	0.0016	0.0015	-0.00002
1500	0.0016	0.0017	0.0016	-0.00007
1300	0.0015	0.0016	0.0015	-0.00002
1100	0.0015	0.0016	0.0014	-0.00007
900	0.0016	0.0016	0.0015	-0.00002
700	0.0016	0.0016	0.0016	-0.00002
500	0.0018	0.0018	0.0017	-0.00004
300	0.0016	0.0016	0.0015	-0.00004
100	0.0016	0.0018	0.0014	-0.00015

(5V-100mA in this device). Fig. 5 shows a schematic of the measurement loop using AO and PSU. In this case, the image of the resistance is created and represented as a voltage.

B. Samples of Collected Data

As seen previously, the load is applied by a pneumatic actuator. It would have been possible to accurately monitor and control the pressure applied to the late, but it has been decided to only monitor the load inside the fibre by means of the load cell and to adapt the calculations accordingly. The load applied varied from 0 to 1500N by increasing steps of 200N with an initial load of 100N. The load has then been decreased from 1500N to 0N by steps of 200N again.

Table I shows the data gathered during a short series of 5 runs on a standard T300 3K fibre. All runs have been realised under similar conditions at a temperature of 100°C by a unique operator. The processed $R - R_0$ column contains the resistance difference in $10^{-6}\Omega$ measured between the loaded fibre and the same unloaded fibre under various loading conditions. The column containing $(R - R_0)/L$ shows the proportionality factor between the processed value of $R - R_0$ and the load. This value is extremely valuable as it is showing the response rate of the sensor to load.

Fig. 5 shows the evolution of $R - R_0$ as a function of the load. Further calculations are presented in Table II (mean, max, min, and standard deviation) allowing the demonstration of the linearity of the response of the sensor to loading.

V. Conclusion

As demonstrated in Table II, the results obtained are showing significant variations when individual runs are isolated, this behaviour is particularly noticeable for loads under 500N. This performance is expected under experimental conditions.

The analysis of the standard deviation of the data is encouraging, in particular for loadings over 700N. As an example, for 5 runs only at 700N, the variations of $(R - R_0)/L$ under the conditions described above are extremely limited.

The successive runs are returning values of 0.00160, 0.00159, 0.00157, 0.00161, and 0.00156 respectively. The percentage of variation is less than 4%, which is promising. Meanwhile, the linearity of the response within each run clearly shows the proportionality of the fibre change of resistance when subjected to loading if it has to be demonstrated.

References

[1] M. Ashby, *Materials Selection in Mechanical Design*, Oxford: Butterworth-Heinemann, 2016.

[2] I. Daniel and O. Ishai, *Engineering Mechanics of Composite Materials*, Oxford University Press, 2006.

[3] W. Haynes, *Handbook of Chemistry and Physics*, Boca Raton, USA: CRC Press, 2011.

[4] F. Mischok, O. Durieux, Y. Vagapov, and D. Fedyashin, "Practical characterisation of the piezo electric properties of a 3K T300 carbon fibre for impact sensoring," in *Proc. IEEE Conf. of Russian Young Researchers in Electrical and Electronic Engineering*, Saint Petersburg, Russia, 29 Jan. - 01 Feb. 2018, pp. 1757-1760, doi: 10.1109/EIConRus.2018.8317446

[5] A. Nag, S. Nuthalapati, and S.C. Mukhopadhyay, "Carbon fiber/ polymer-based composites for wearable sensors: A review," *IEEE Sensors Journal*, vol. 22, no. 11, pp. 10235-10245, 2022, doi: 10.1109/JSEN.2022.3170313

[6] N. Forintos, T. Sarkadi, O.C. Boros, and T. Czigany, "Multifunctional carbon fiber sensors: The effect of anisotropic electrical conductivity," *IEEE Sensors Journal*, vol. 21, no. 7, pp. 8960-8968, 2021, doi: 10.1109/JSEN.2021.3053125

[7] J. Jang, S. Kim, K. Lee, S. Park, G.-Y. Park, B.-J. Kim, J. Oh, and M.J. Lee, "Knitted strain sensor with carbon fiber and aluminum-coated yarn, for wearable electronics," *Journal of Materials Chemistry C*, vol. 9, no. 46, pp. 16440-16449, Dec. 2021, doi: 10.1039/D1TC01899J

[8] H.D. Roh and Y.-B. Park, "Carbon fiber grid sensor for structural deformation using piezoresistive behavior of carbon fiber," *Sensors and Actuators: A. Physical*, vol. 341, 2022, Art no. 113348, doi: 10.1016/j.sna.2021.113348

[9] J. Zhu, X. Xue, J. Li, J. Wang, H. Wang, Y. Xing, and P. Zhu, "Flexible pressure sensor with a wide pressure measurement range and an agile response based on multiscale carbon fibers/carbon nanotubes composite," *Microelectronic Engineering*, vol. 257, 2022, Art no. 111750, 10.1016/j.mee.2022.111750

[10] J.M. Ziman, "A theory of the electrical properties of liquid metals. I: The monovalent metals," *The Philosophical Magazine: A Journal of Theoretical Experimental and Applied Physics*, vol. 6, no. 68, pp. 1013-1034, 1961, doi: 10.1080/14786436108243361

[11] R. Mueller, K. Agyeman, and C. Tsuei, "Negative-temperature coefficients of electrical resistivity in amorphous La-based alloys," *Physical Review B*, vol. 22, no. 6, pp. 2665-2669, 1980, doi: 10.1103/ PhysRevB.22.2665

[12] J. Ullrich, M. Eisenreich, Y. Zimmermann, D. Mayer, N. Koehne, J.F. Tschannett, A. Mahmud-Ali, and T. Bechtold, "Piezo-sensitive fabrics from carbon black containing conductive cellulose fibres for flexible pressure sensors," *Materials*, vol. 13, no. 22, Nov. 2020, Art no. 5150, doi: doi:10.3390/ma13225150

[13] N. Schmidova, J. Macken, A. Horoschenkoff, R. Sedlacek, T. Kostroun, J. Simota, and M. Ruzicka, "Impact damage detection of a glass fabric composite using carbon fiber sensors with regard to mechanical loading," *Applied Sciences*, vo. 12, no. 3, Jan. 2022, Art no. 1112, doi: 10.3390/app12031112

[14] Y. Wan, W. Hu, L. Yang, Z. Wang, J. Tan, Y. Liu, F. Wang, B. Yang, "In-situ monitoring of glass fiber/epoxy composites by the embedded multi-walled carbon nanotube coated glass fiber sensor: From fabrication to application," *Polymer Composites*, vol. 43, no. 7, pp. 4210-4222, July 2022, doi: 10.1002/pc.26682

[15] Y. Varshni, "Temperature dependence of the elastic constants," *Physical Review B*, vol. 2, no. 10, pp. 3952-3958, 1970, doi: 10.1103/ PhysRevB.2.3952